

Research Paper

Transport Mechanisms of Carnosine in SKPT Cells: Contribution of Apical and Basolateral Membrane Transporters

Dilara Jappar,¹ Yongjun Hu,¹ Richard F. Keep,^{2,3} and David E. Smith^{1,4,5}

Received May 8, 2008; accepted September 8, 2008; published online September 27, 2008

Purpose. The aim of this study was to investigate the transport properties of carnosine in kidney using SKPT cell cultures as a model of proximal tubular transport, and to isolate the functional activities of renal apical and basolateral transporters in this process.

Methods. The membrane transport kinetics of 10 μM [³H]carnosine was studied in SKPT cells as a function of time, pH, potential inhibitors and substrate concentration. A cellular compartment model was constructed in which the influx, efflux and transepithelial clearances of carnosine were determined. Peptide transporter expression was probed by RT-PCR.

Results. Carnosine uptake was 15-fold greater from the apical than basolateral surface of SKPT cells. However, the apical-to-basolateral transepithelial transport of carnosine was severely rate-limited by its cellular efflux across the basolateral membrane. The high-affinity, proton-dependence, concentration-dependence and inhibitor specificity of carnosine supports the contention that PEPT2 is responsible for its apical uptake. In contrast, the basolateral transporter is saturable, inhibited by PEPT2 substrates but non-concentrative, thereby, suggesting a facilitative carrier.

Conclusions. Carnosine is expected to have a substantial cellular accumulation in kidney but minimal tubular reabsorption in blood because of its high influx clearance across apical membranes by PEPT2 and very low efflux clearance across basolateral membranes.

KEY WORDS: carnosine; cellular kinetics; PEPT2; SKPT; transport mechanisms.

INTRODUCTION

Proton-coupled oligopeptide transporters (POTs) are membrane proteins that translocate various small peptides and peptide-like drugs across the biological membrane *via* an inwardly-directed proton gradient and negative membrane potential. At present, four members of the POT family, namely PEPT1, PEPT2, PHT1 and PHT2, have been identified in mammals (1,2). POTs have significant physio-

logical roles in the absorption and reabsorption of peptide-bound amino nitrogen as well as pharmacological roles in drug absorption and disposition (e.g., β -lactam antibiotics, angiotensin-converting enzyme inhibitors, renin inhibitors, bestatin and valacyclovir). PEPT1, cloned from a rabbit small intestine cDNA library (3), has been characterized as a high-capacity, low-affinity transporter. In addition to its expression in apical membranes of S1 segments in proximal tubule (i.e., kidney cortex), PEPT1 is highly expressed in apical membranes of small intestine (4,5). PEPT2, cloned from a human kidney cDNA library (6), is a low-capacity, high-affinity transporter that is primarily localized in the brush border of S3 segments in proximal tubule (i.e., outer stripe of outer medulla) (4,6,7), as well as in brain, choroid plexus, eye, lung and mammary gland (8). In spite of the sequential expression of PEPT1 and PEPT2 in renal proximal tubules, studies have definitively shown that PEPT2 accounts for the vast majority of reabsorption for the model dipeptide glycylsarcosine (GlySar) and the β -lactam antibiotic cefadroxil in kidney (9–12).

Two additional peptide transporters, PHT1 (13) and PHT2 (14), have been cloned from a rat brain cDNA library. Unlike PEPT1 and PEPT2, they transport a single amino acid, L-histidine, in addition to the proton-stimulated transport of di/tripeptides. While PHT1 mRNA is abundantly expressed in rat brain and eye, PHT2 mRNA is abundant in rat lung, spleen, thymus and immunocytes. Unlike other POT family members, PHT2 protein was found subcellularly in the lysosomes of transfected cell lines rather than in the plasma

Electronic supplementary material The online version of this article (doi:10.1007/s11095-008-9726-9) contains supplementary material, which is available to authorized users.

¹ Department of Pharmaceutical Sciences, University of Michigan, Ann Arbor, Michigan 48109, USA.

² Department of Neurosurgery, University of Michigan, Ann Arbor, Michigan 48109, USA.

³ Department of Physiology, University of Michigan, Ann Arbor, Michigan 48109, USA.

⁴ University of Michigan, Upjohn Center for Clinical Pharmacology, 4742 Medical Sciences II, 1150 W. Medical Center Drive, Ann Arbor, Michigan 48109-5633, USA.

⁵ To whom correspondence should be addressed. (e-mail: smithb@umich.edu)

ABBREVIATIONS: GAPDH, glyceraldehyde 3-phosphate dehydrogenase; GlySar, glycylsarcosine; PEPT, peptide transporter; PHT, peptide/histidine transporter; POTs, proton-coupled oligopeptide transporters; SKPT, spontaneous hypertensive rat kidney proximal tubule.

membrane, as demonstrated by light and electron-microscopic analyses (14). Compared to PEPT1 and PEPT2, relatively little is known about PHT1 and PHT2 with respect to their physiological roles, substrate specificities, precise localization and directionality of transport.

Functional studies have indicated the presence of distinct basolateral peptide transporters in the small intestine (15) and kidney (16). In this regard, the intestinal basolateral peptide transporter, expressed in the Caco-2 cells, was suggested as a facilitative efflux transporter that assists in the efficient absorption of small peptides/mimetics by mediating their extrusion from cell to blood (15,17,18). In contrast, the renal basolateral peptide transporter, expressed in MDCK cells, was suggested as an influx transporter facilitating the clearance of small peptides/mimetics from the blood circulation (18). Thus far, none of these basolateral peptide transporters have been cloned and, hence, they are not well characterized compared to current members of the POT family.

Carnosine (β -alanyl-L-histidine) is a naturally-occurring dipeptide that is highly concentrated in skeletal muscle and brain. Besides being an endogenous substrate, carnosine is also taken exogenously as a dietary supplement for its antioxidant and free radical scavenging properties (19,20). In the body, carnosine prevents glycation and the cross-linking of proteins by deleterious aldehydes and ketones (21), further protecting the cell against oxidative damage. The potential benefit of carnosine is limited by its susceptibility to hydrolysis by tissue and serum carnosinase, but not α -peptidase (22), resulting in degradation to its constituent amino acids (i.e., β -alanine and L-histidine). Pharmacologically, carnosine has some renoprotective effects including acting as a protective factor in diabetic nephropathy (23) and preventing ischemia-induced renal injury (24–26). Carnosine is transported by all of the POTs (13,14,27–29).

Even though carnosine has significant pharmacological importance in the kidney, the renal disposition of this dipeptide has not been elucidated. Therefore, the aim of this study was to investigate the transport properties of carnosine in kidney using SKPT cell cultures as a model of proximal tubular transport, and to isolate the functional activities of renal apical and basolateral transporters in this process.

MATERIALS AND METHODS

Reagents

[³H]Carnosine (10 Ci/mmol) and [¹⁴C]D-mannitol (53 mCi/mmol) were purchased from Moravak Biochemicals (Brea, CA). Primers for the PCR analyses were obtained from Invitrogen Life Technologies (Carlsbad, CA). The epithelial cell line SKPT-0193 C1.2, established by SV40 transformation of isolated rat kidney proximal tubule cells, was kindly provided by Dr. Ulrich Hopfer (Case Western Reserve University, Cleveland, OH). All other chemicals were from standard sources and were of the highest quality available.

Cell Cultures

SKPT cells were grown on 75 cm² cell culture flasks and cultured in 1:1 DMEM (without glucose)/HAM'S F12 medium supplemented with 5% fetal bovine serum, 5 μ g/mL

apotransferrin, 5 μ g/mL insulin, 4 μ g/mL dexamethasone, 10 ng/mL epidermal growth factor, 15 mM HEPES, 0.06% NaHCO₃, 50 μ M ascorbic acid, 20 nM selenium and 1% penicillin G (100 U/mL)/streptomycin (100 μ g/mL). As described previously (30), cells were subcultured every 3–5 days by treatment with 0.05% trypsin and 0.53 mM EDTA at 37°C. SKPT cells were seeded on collagen-coated (5 μ g/cm²) 12-transwell filter inserts (12 mm diameter, 0.4 μ m pore size) at 10⁵ cells/well density (10⁵ cell/cm²), and the culture medium was changed every other day. At 24 h prior to experimentation, antibiotics were removed from the culture medium. SKPT cells were used 4 days after the initial seeding. Transepithelial electrical resistance was measured prior to the experiments to ensure the integrity of cell monolayers.

Reverse Transcription-Polymerase Chain Reaction (RT-PCR) Analyses

RT-PCR was used to identify the expression of specific POT mRNA in SKPT cells. In brief, total RNA was isolated from SKPT cells using an RNeasy Mini Kit (Qiagen, Valencia, CA). The RNA was then reverse-transcribed in a 40 μ L reaction mixture containing 200 U of Moloney murine leukemia virus reverse transcriptase and random primers. cDNA was amplified with specific primers for all four oligopeptide transporters by PCR. The primers were designed using the Vector NTI program (Invitrogen, Carlsbad, CA), and PCR was performed in a 60- μ L reaction mixture containing 2 U of *Taq* DNA polymerase, 4 pmol each of the 5' and 3' primers for each POT, 0.2 μ g of cDNA sample, 1.5 mM MgCl₂, and 0.5 mM deoxytriphosphate nucleotide mixture. Glyceraldehyde 3-phosphate dehydrogenase (GAPDH) was used as a control for PCR analyses. The positive controls for oligopeptide transporters were rat small intestine (PEPT1), rat kidney (PEPT2), and rat brain (PHT1 and PHT2). The amplified products were separated on a 1.5% agarose gel and visualized with ethidium bromide. Primers and PCR conditions for each POT are listed in the supplementary material (Table I of the Electronic supplementary material).

Carnosine Intracellular Accumulation and Transepithelial Transport Studies

The uptake buffer consisted of 25 mM MES/Tris (pH 6.0) or 25 mM HEPES/Tris (pH 7.4), each containing 140 mM NaCl, 5.4 mM KCl, 1.8 mM CaCl₂, 0.8 mM MgSO₄ and 5 mM glucose. For intracellular accumulation and transepithelial transport experiments, the cell monolayers were washed and preincubated apically with 0.4 mL of pH 6.0 buffer and basolaterally with 1.2 mL of pH 7.4 buffer for 10 min at 37°C. The buffers were then removed and fresh buffer (0.4 mL pH 6.0 or 1.2 mL pH 7.4 containing [³H] carnosine and [¹⁴C]mannitol; 10 μ M each) was added to the apical or basolateral compartments, respectively, in the absence and presence of potential inhibitors. Control buffer of 1.2 mL pH 7.4 or 0.4 mL pH 6.0 was added to the opposite compartment (i.e., no carnosine, mannitol or inhibitor). Cells were then incubated for the indicated length of time at 37°C. For transepithelial flux experiments, a 100- μ L aliquot was collected from the opposite compartment from where drug was placed, and the radioactivity counted. For intracellular

accumulation experiments, media were aspirated from both compartments and the monolayers were then washed four times from both sides with ice-cold buffer. The filters with monolayers were detached from the chamber, placed in a scintillation vial, and the cells were solubilized with 0.2 M NaOH and 1% SDS. Radioactivity was measured in solubilized cells (and buffer) with a dual-channel liquid scintillation counter (Beckman LS 6000 SC; Beckman Coulter Inc., Fullerton, CA). Protein concentrations were measured using the Bio-Rad DC protein assay (Bio-Rad Laboratories, Hercules, CA) with bovine serum albumin as the standard. Mannitol was used to correct the uptake data of carnosine due to filter binding and extracellular content (28,31), as well as the transepithelial transport of carnosine due to paracellular flux (32).

Determination of Intracellular Volume

The intracellular volume of SKPT cells was measured by the 3-*O*-methyl-D-glucose method (33,34) in glucose-free media. The cell monolayers were washed and preincubated apically with 0.4 mL of pH 6.0 buffer and basolaterally with 1.2 mL of pH 7.4 buffer for 10 min at 37°C. The buffers were then removed and fresh buffer (0.4 mL pH 6.0 or 1.2 mL pH 7.4 containing [³H]3-*O*-methyl-D-glucose and [¹⁴C]mannitol; 1 mM, 5 mM, and 10 mM of each) was added to the apical and basolateral compartments, respectively, in presence of 200 μM of phloridzin (an inhibitor of Na⁺-coupled glucose cotransport). After 300 min of incubation at 37°C, the uptake buffers were aspirated from both compartments and the monolayers were washed five times from both sides with ice-cold buffer containing 100 μM of phloretin (an inhibitor of facilitated diffusion). The filters with monolayers were then detached from the chamber, placed in a scintillation vial, and the cells were solubilized with 0.2 M NaOH and 1% SDS. Radioactivity was measured in solubilized cells with a dual-channel liquid scintillation counter (Beckman LS 6000 SC; Beckman Coulter Inc., Fullerton, CA). Uptake of 3-*O*-methyl-D-glucose was normalized for amount of protein per well, and the slope of uptake vs. concentration was taken as the intracellular volume of SKPT cells.

Efflux Studies

SKPT monolayers were loaded by incubating the cells apically with [³H]carnosine and [¹⁴C]mannitol (10 μM each) for 2 h at 37°C. Following incubation, monolayers were washed four times from both sides with ice-cold buffer (no substrate present). The monolayers were then incubated at 37°C with control buffer in both compartments (i.e., 0.4 mL of pH 6.0 buffer in the apical side and 1.2 mL of pH 7.4 buffer in the basolateral side). At specified times, 100 and 300 μL aliquots were taken from the apical and basolateral compartments, respectively, and replaced with fresh buffer. Radioactivity was measured in the buffer samples with a dual-channel liquid scintillation counter, and efflux was expressed as a percentage relative to carnosine's initial concentration in cells after the 2-h loading period.

Substrate Stability Studies

Carnosine stability was evaluated in the apical, basolateral and intracellular compartments of SKPT cells. Following apical

or basolateral incubations of [³H]carnosine (10 μM) for 5, 10, 15, 60, 120, 180 and 300 min at 37°C, media were collected from the donor and receiver sides for analysis. The monolayers were washed four times with ice-cold buffer, and the filters with monolayers were detached from the chamber. The cells were mixed with 0.5 mL of Milli-Q water and then lysed by sonication for 30 s × 5 times. An equal volume of acetonitrile was added to the cell lysates, vortexed for 5 s, and centrifuged at 14,000 × *g* for 10 min at 4°C. Cell supernatants were concentrated under cryovacuum (SpeedVac concentrator SVC 200H with Refrigerated Condensation Trap RT 4104, Savant Instrument Inc, Farmingdale, NY) and analyzed, along with buffer samples, by high-performance liquid chromatography (Model 515 Pump, Water, Milford, MA) with radiochromatography detection (Flo-One 500TR, PerkinElmer Life and Analytical Sciences, Boston, MA). Sample components were separated using a reversed-phase column (Supelco Discovery® C-18, 5 μm, 250 cm × 4.6 mm, Supelco Park, Bellefonte, PA) subjected to a mobile phase of 0.1 M NaH₂PO₄ and 0.075% heptafluorobutyric acid, pumped isocratically at 1 mL/min. Retention times for histidine and carnosine were 4.4 and 7.9 min, respectively, under ambient conditions. Carnosine stability was determined by its recovery and the appearance of histidine following the specified incubation periods.

Kinetic Analyses

The influx and efflux clearances of carnosine across SKPT cell membranes are depicted by the three-compartment model in Fig. 1A. Variations in the amount of carnosine with time are described in each compartment according to the following mass balance equations (35):

$$\frac{dX_A}{dt} = CL_{CA} \times C_C - CL_{AC} \times C_A \quad (1)$$

$$\frac{dX_B}{dt} = CL_{CB} \times C_C - CL_{BC} \times C_B \quad (2)$$

$$\frac{dX_C}{dt} = CL_{AC} \times C_A + CL_{BC} \times C_B - (CL_{CA} + CL_{CB}) \times C_C \quad (3)$$

where X_A , X_B and X_C (picomoles per milligram of protein) are the amounts of carnosine, respectively, in the apical, basolateral and cellular compartments; C_A , C_B and C_C (picomoles per microliter) are the respective concentrations of carnosine in the apical, basolateral and cellular compartments; CL_{AC} and CL_{BC} (microliters per minute per milligram of protein) represent the influx clearances from the apical and basolateral compartments, respectively, to the cellular compartment; and CL_{CA} and CL_{CB} represent the respective efflux clearances from the cellular compartment to the apical and basolateral compartments. The transepithelial transport of carnosine is depicted in Fig. 1B and can be described by:

$$\frac{dX_A}{dt} = CL_{BA} \times C_B \quad \text{B - to - A directional transport} \quad (4)$$

$$\frac{dX_B}{dt} = CL_{AB} \times C_A \quad \text{A - to - B directional transport} \quad (5)$$

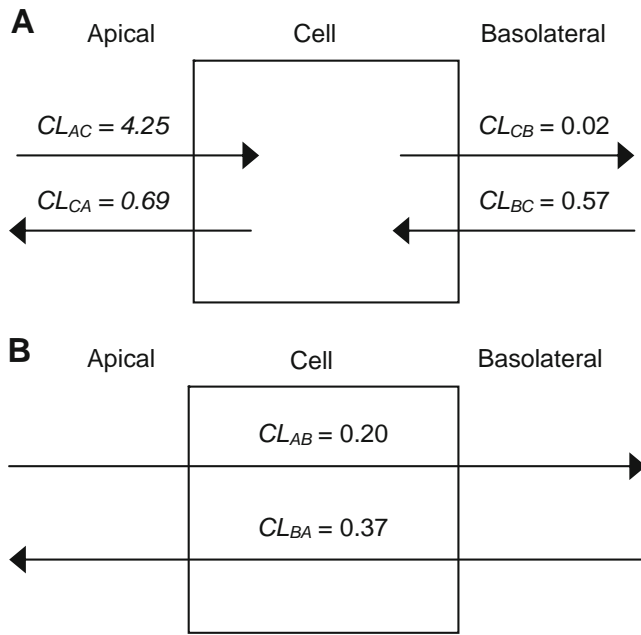


Fig. 1. Schematic representation of the SKPT cellular model in which CL_{AC} and CL_{BC} represent the influx clearances from the apical and basolateral compartments, respectively, while CL_{CA} and CL_{CB} represent the respective efflux clearances to the apical and basolateral compartments (**A**); CL_{AB} represents the apical-to-basolateral transepithelial clearance and CL_{BA} represents the basolateral-to-apical transepithelial clearance (**B**). The clearance values are those determined experimentally for carnosine in this study (units, microliters per milligram per minute).

where CL_{AB} and CL_{BA} represent the transcellular clearances of carnosine from the apical to basolateral compartment and from the basolateral to apical compartment, respectively. Finally, the transcellular clearance can be described by:

$$CL_{AB} = CL_{AC} \times f_{\text{efflux.B}} \quad (6)$$

$$CL_{BA} = CL_{BC} \times f_{\text{efflux.A}} \quad (7)$$

where $f_{\text{efflux.A}}$ and $f_{\text{efflux.B}}$ represent the fraction of carnosine effluxed from the cellular compartment to the apical and basolateral compartments, respectively, at steady state.

A Michaelis–Menten model was used to fit the concentration-dependent uptake data of carnosine, where V is the initial uptake rate, V_{max} is the maximal rate of saturable uptake, K_m is the Michaelis constant, and S is the substrate concentration (Eq. 8). The unknown parameters (i.e., V_{max} and K_m) were determined by nonlinear regression analysis (GraphPad Prism v4.0; GraphPad Software, Inc. San Diego, CA) and a weighting factor of unity. The quality of fit was determined by evaluating the coefficient of determination (r^2), the standard error of parameter estimates, and the residual plots:

$$V = \frac{V_{\text{max}} \times S}{K_m + S} \quad (8)$$

While other transport models were attempted (i.e., saturable component plus linear term; two saturable components), they did not fit the data as well as a saturable component alone.

Statistical Analyses

All data were reported as mean \pm SE. Cellular uptakes of carnosine were standardized for the total amount of protein (milligrams) in SKPT cells. Statistical differences were determined between groups by analysis of variance followed by Dunnett's test for pairwise comparisons with the control group (GraphPad Prism, v4.0; GraphPad Software, Inc., La Jolla, CA). A probability of $p \leq 0.05$ was considered significant.

RESULTS

RT-PCR Analyses of POT Expression in SKPT Cells

Specific POT transcripts were sought in SKPT cells and kidney lysates (Fig. 2), while intestinal lysates served as a positive control for PEPT1 mRNA and brain lysates served as a positive control for PHT1 or PHT2 mRNA. Although kidney lysates expressed all four members of the POT family, only PEPT2 and PHT1 transcripts were expressed in SKPT cells. GAPDH, which served as a housekeeper gene, was strongly expressed in all samples. Given the predominant role of PEPT2 in renal reabsorption (9–12), the presence of PEPT2 mRNA in SKPT cells suggests that this cell line was a good model to study the proximal tubular transport of peptides (e.g., carnosine) in kidney. The presence of PHT1 mRNA in SKPT cells also allows us to evaluate whether this peptide–histidine transporter has a functional role in the disposition of small peptides in kidney.

Time Course of Carnosine Intracellular Accumulation and Transepithelial Transport

As observed in Fig. 3A, the apical uptake of carnosine was substantially greater than its uptake from the basolateral surface of SKPT cell monolayers (≈ 15 -fold). It was also observed that carnosine uptake was linear for 60 min at the apical surface and for 30 min at the basolateral surface. As a result, initial rates were determined at 15 min for both apical and basolateral uptakes in subsequent experiments. At 180–300 min, the apical uptake of carnosine reached a plateau value of approximately 220 pmol/mg protein. Using the experimentally determined value for intracellular volume of SKPT cells (i.e., $2.0 \pm 0.1 \mu\text{L/mg}$ of protein), and given that the extracellular medium concentration of carnosine was 10 μM , the intracellular to extracellular concentration ratio of carnosine was 11, indicating the presence of active uptake process(es) at the apical membrane (possibly PEPT2 and/or PHT1). However, when carnosine was introduced from the basolateral compartment, the uptake reached a plateau value of only 15 pmol/mg protein. This result translated into an intracellular to extracellular concentration ratio of only 0.8, indicating the absence of a concentrative mechanism for carnosine uptake at the basolateral membrane.

In contrast to its intracellular accumulation, the apical-to-basolateral transcellular flux of carnosine was smaller than its basolateral-to-apical transcellular flux (≈ 2 -fold) (Fig. 3B). This finding suggests that although carnosine preferentially accumulates in the cell from the apical surface, its basolateral efflux is very limited thereby driving carnosine back to the

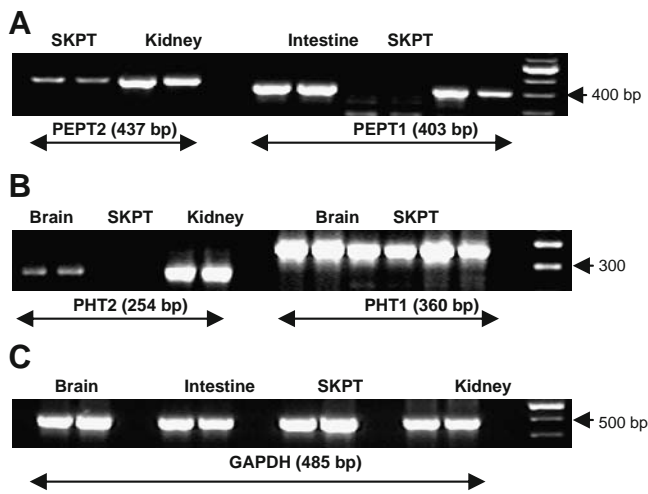


Fig. 2. RT-PCR analysis of peptide transporter mRNA in SKPT cells, and in kidney, intestine and brain lysates (4 μ g total RNA). Samples were separated on a 1.5% agarose gel, visualized with ethidium bromide, and screened for PEPT1 and PEPT2 transcripts (A) and for PHT1 and PHT2 transcripts (B). GAPDH controls for rat brain, intestine, kidney and SKPT cDNA samples are also displayed (C). In each gel, the *right-hand lane* is a 100-bp DNA ladder. The expected RT-PCR products are shown for each POT under the gel.

apical compartment. This aspect is further examined in the efflux studies below.

Efflux of Carnosine

In order to test our interpretation of the transcellular transport data and to better understand the fate of carnosine once inside the cell, the efflux of carnosine was evaluated after 2 h of apical preloading. As shown in Fig. 3C, about 40% of carnosine was effluxed from the cell to the apical compartment at 60 min and about 4% of cellular carnosine was effluxed to the basolateral compartment. When a single exponential term was used to fit the efflux-time profile [i.e., $Y = Y_{ss} \times (1 - e^{-K_{eff} \times t})$], we found that 66% of carnosine was effluxed from the cellular to apical compartment while only 4.7% of carnosine was effluxed to the basolateral compartment at steady state (i.e., $f_{efflux,A} = 0.66$ and $f_{efflux,B} = 0.047$, respectively). This finding is in accordance with the transepithelial transport data, which suggested a very minimal efflux of carnosine across the basolateral membrane.

Kinetics Analysis of Carnosine Cellular Transport

Based on the slopes of the transport *versus* time profiles depicted in Fig. 3B, the A-to-B transepithelial rate of carnosine was 1.99 pmol/min/mg protein while the B-to-A transepithelial rate of carnosine was 3.74 pmol/min/mg protein. Given that these studies were performed with 10 μ M concentrations in the donor compartment, and according to Eqs. 4 and 5, the transepithelial clearances were calculated as: $CL_{AB} = 0.20 \mu\text{L}/\text{min}/\text{mg}$ and $CL_{BA} = 0.37 \mu\text{L}/\text{min}/\text{mg}$. With a knowledge of the fractional effluxes of carnosine to both apical and basolateral compartments (see efflux studies above), and the transepithelial clearances determined here, the influx clearances of carnosine were determined according to Eqs. 6 and 7, in

which: $CL_{AC} = 4.25 \mu\text{L}/\text{min}/\text{mg}$ and $CL_{BC} = 0.57 \mu\text{L}/\text{min}/\text{mg}$. Finally, the efflux clearances of carnosine were calculated according to Eqs. 1 and 2 (now that all other parameters are known), such that: $CL_{CA} = 0.69 \mu\text{L}/\text{min}/\text{mg}$ and $CL_{CB} = 0.018 \mu\text{L}/\text{min}/\text{mg}$. All clearance values are summarized in the cellular models shown in Fig. 1.

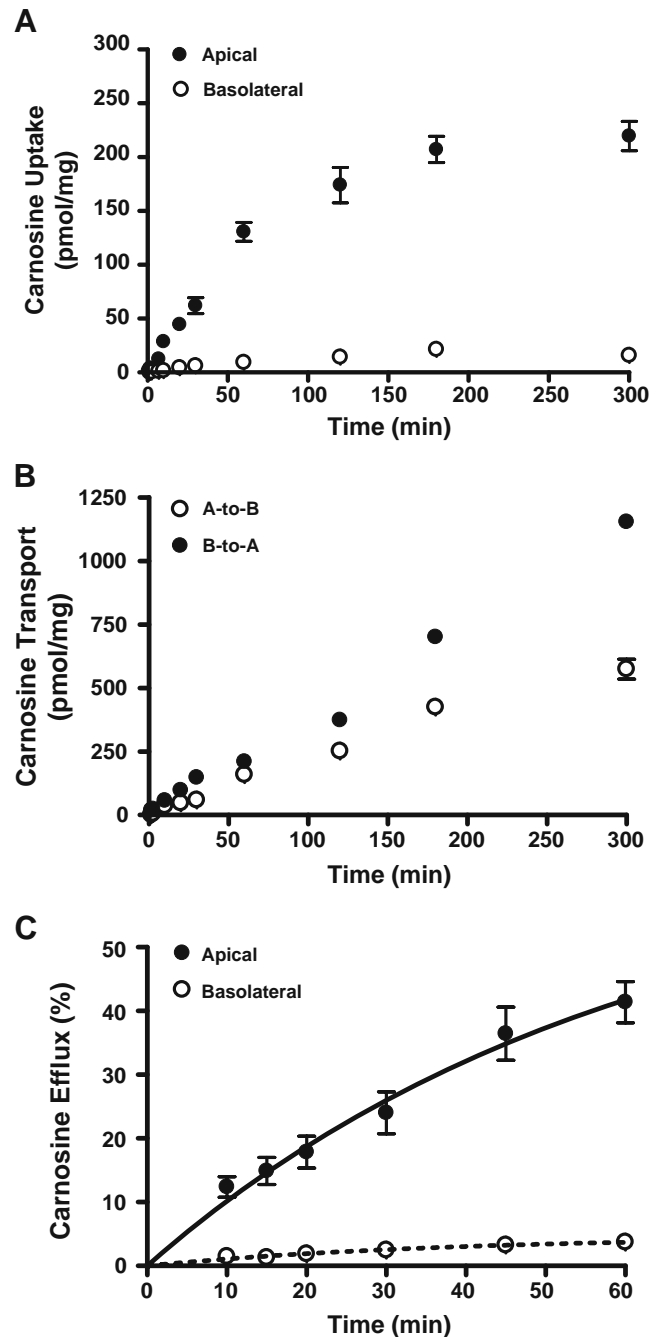


Fig. 3. Intracellular accumulation (A) and transcellular transport (B) of 10 μ M [^3H]carnosine as a function of time in SKPT cell monolayers at 37°C. The cellular efflux (C) of [^3H]carnosine was determined after preloading the cells from the apical side with 10 μ M carnosine for 2 h at 37°C. For all experiments, the buffer pH was 6.0 in the apical compartment and 7.4 in the basolateral compartment. Data are expressed as mean \pm SE ($n = 3-5$).

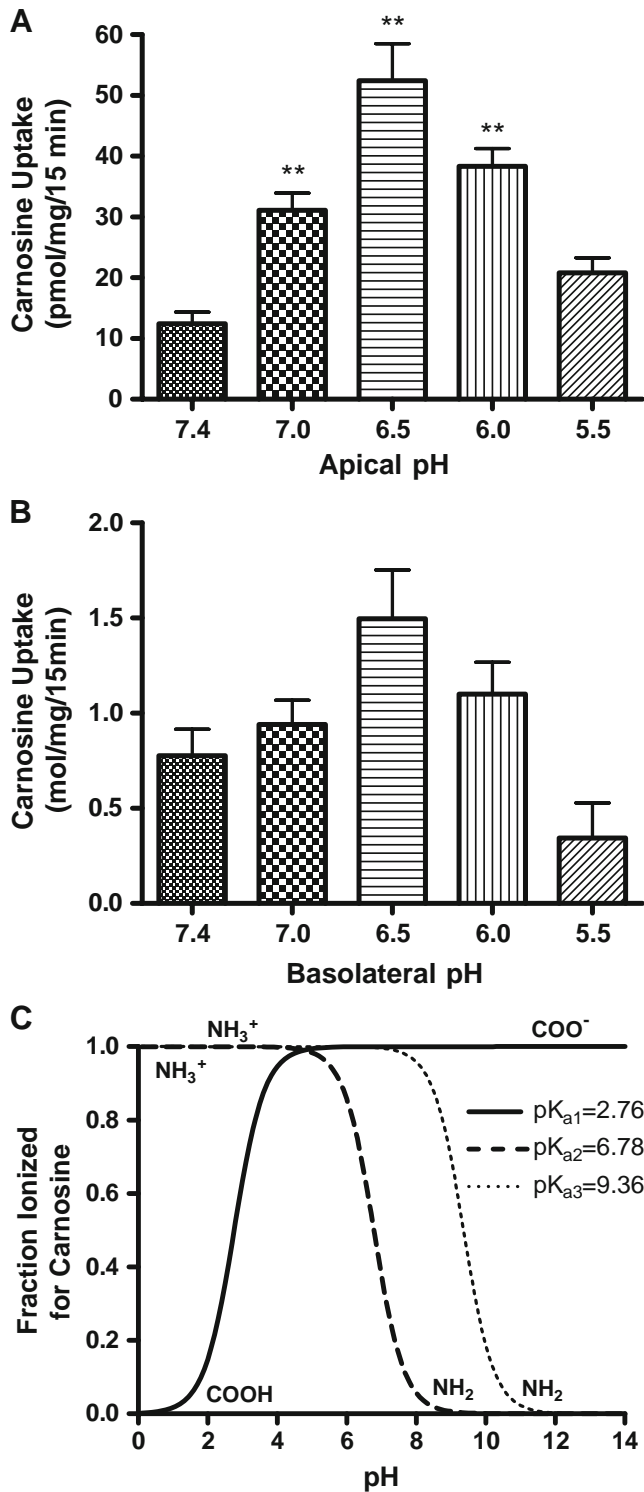


Fig. 4. Effect of pH on the 15-min uptake of 10 μM [^3H] carnosine in SKPT cell monolayers at 37°C from the apical (A) compartment (basolateral pH maintained at 7.4) and from the basolateral (B) compartment (apical pH maintained at 6.0). Data are expressed as mean \pm SE ($n=3-6$). ** $p < 0.01$, as compared to pH 7.4. Relationship between pH and fractional ionization of carnosine (C).

Proton-Dependent Uptake of Carnosine

To determine whether the uptake of carnosine was stimulated by an inwardly-directed proton gradient, we

evaluated the uptake of carnosine from both membrane surfaces at various pH values. This was achieved by varying pH of the donor side from 5.5 to 7.4 while keeping the apical side at pH 6.0 for basolateral uptakes and the basolateral side at pH 7.4 for apical uptakes. As shown in Fig. 4A, the apical uptake of carnosine demonstrated a marked dependency on extracellular pH values and was maximal at pH 6.5, which is consistent with the proton-substrate symport characteristics of the PEPT2 and PHT1. In contrast, the basolateral uptake of carnosine (Fig. 4B) was more insensitive to changes in external pH (maximal at pH 6.5; $p > 0.05$ for all comparisons). Carnosine is a basic dipeptide with pK_a values of 2.76, 6.78 and 9.36 (36). Therefore, as the pH of the environment increases from 5.5 to 7.4, carnosine becomes less basic

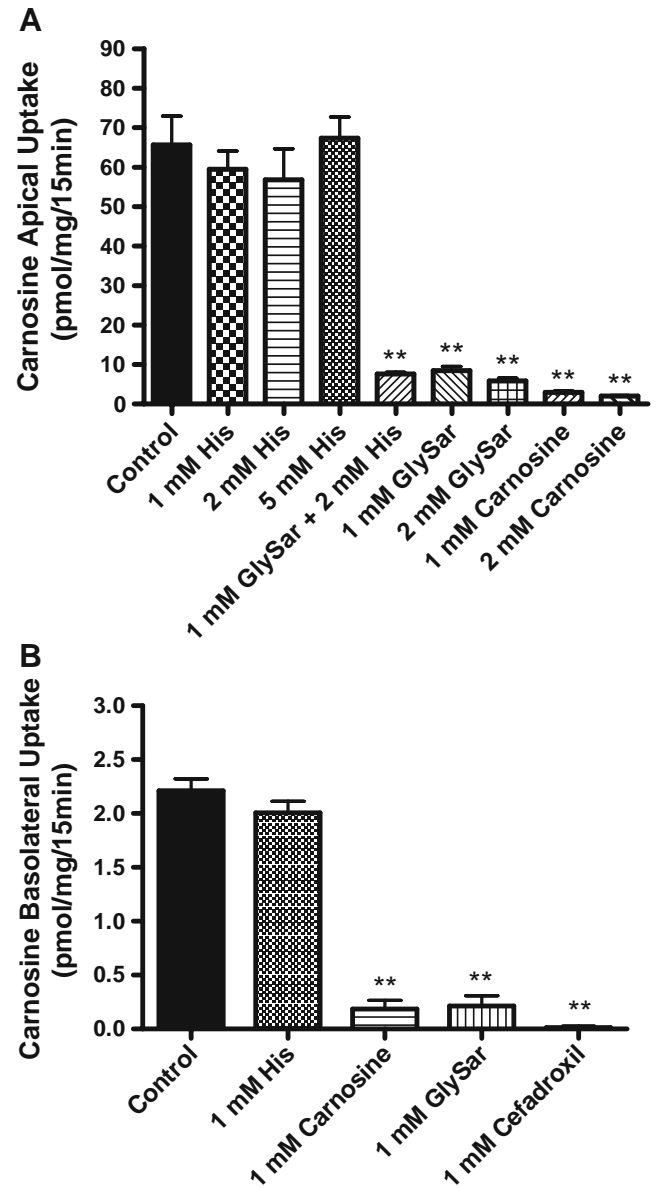


Fig. 5. Effect of potential inhibitors on the 15-min apical (A) and basolateral (B) uptake of carnosine in SKPT cell monolayers at 37°C. For all experiments, the buffer pH was 6.0 in the apical compartment and 7.4 in the basolateral compartment. Data are expressed as mean \pm SE ($n=3-6$). ** $p < 0.01$, as compared to control.

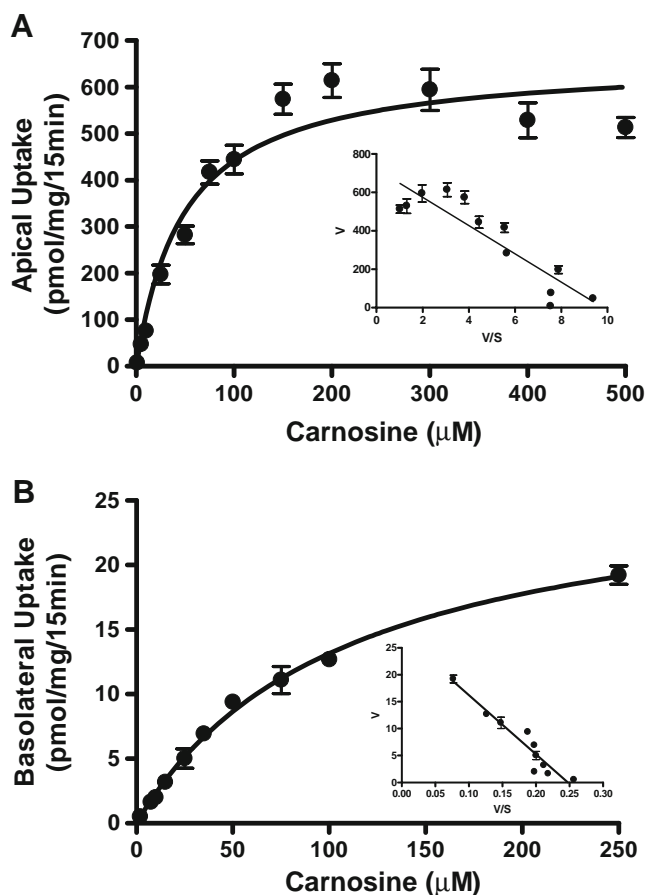


Fig. 6. Effect of concentration on the 15-min uptake of 1–500 μM [^3H]carnosine from the apical (A) and basolateral (B) sides of SKPT cell monolayers at 37°C. For all experiments, the buffer pH was 6.0 in the apical compartment and 7.4 in the basolateral compartment. Data are presented as mean \pm SE ($n=3-6$); the inset is a Woolf-Augustinsson-Hofstee plot of the transformed data (V , picomoles per milligram per 15 min versus V/S , microliters per milligram per 15 min).

(Fig. 4C). Thus, at pH 5.5 carnosine is 95% ionized (NH_3^+), at pH 6.5 carnosine is 65% ionized (NH_3^+), and at pH 7.4 carnosine is 15–20% ionized (NH_3^+). While higher pH values would favor an increased passive uptake of carnosine, the PEPT2-mediated uptake of dipeptide is not favored due to a reduction in proton motive force. Moreover, pH may also affect the protonation state of the peptide transporter protein. The multiple influences of pH, along with membrane potential, should be considered when drawing conclusions about peptide transporter activity.

Effect of Potential Inhibitors

Specificity of carnosine transport at the apical and basolateral membranes of SKPT cells was evaluated by co-incubating the substrate with potential inhibitors. In particular, the PEPT2-mediated uptake of carnosine was probed by performing studies in the absence and presence of GlySar, while the PHT1-mediated uptake of carnosine was probed with histidine. As shown in Fig. 5A, the apical uptake of carnosine was unaffected by 1, 2 and 5 mM of histidine (a potent inhibitor of PHT1). In contrast, 1 and 2 mM of GlySar

(a classic inhibitor of PEPT2) reduced the apical uptake of carnosine by 90%. Self-inhibition experiments revealed that 1 and 2 mM of unlabeled substrate inhibited the apical uptake of radiolabeled carnosine by 96%. At the basolateral membrane, carnosine uptake was unaffected by 1 mM of histidine but reduced by 90–99% in the presence of 1 mM of GlySar, unlabeled carnosine (self-inhibition), or cefadroxil (Fig. 5B).

Concentration-Dependent Uptake of Carnosine

The concentration dependency of carnosine was characterized at both the apical and basolateral surfaces of SKPT cells. At the apical membrane, carnosine uptake was saturable (Fig. 6A) with Michaelis-Menten parameters of $V_{\text{max}}=659\pm 27$ pmol/mg/15 min and $K_m=49\pm 8$ μM . Carnosine was also found to have saturable transport kinetics at the basolateral membrane (Fig. 6B) where the $V_{\text{max}}=27.4\pm 1.3$ pmol/mg/15 min and $K_m=108\pm 10$ μM . Linear transformations of the data, as shown in Woolf-Augustinsson-Hofstee plot inserts, suggest the involvement of a single specific transporter for the uptake of carnosine at each membrane. However, compared to the apical transporter (i.e., PEPT2), the basolateral transporter has a 24-fold lower capacity and a twofold lower affinity. The results are consistent with the previous cellular accumulation, transepithelial transport and pH-dependent findings, in which different transport systems appear to be involved for carnosine at the apical and basolateral membranes of SKPT cells.

Stability of Carnosine

As shown in Fig. 7, carnosine remained intact in the donor compartment, whether introduced from the apical or basolateral side, for up to 300 min of incubation. However, there was some degradation of carnosine in the intracellular compartment after the first hour of incubation. In this regard, carnosine was >94% intact for the first 15 min of incubation while being about 87% intact at 60 min and 81% intact at 300 min of incubation. Overall, these findings indicate that carnosine was mostly intact during the intracellular accumu-

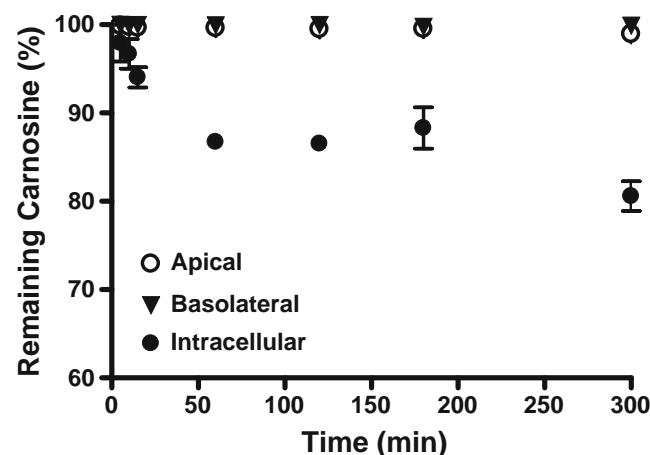


Fig. 7. Stability of [^3H]carnosine in the apical, basolateral, and intracellular compartments of SKPT cell monolayers as a function of time (pH 6.0 buffer in apical side and pH 7.4 buffer in basolateral side). Data are presented as mean \pm SE ($n=3$).

lation, transepithelial transport and efflux experiments, and completely stable for those experiments in which incubation times were only 15 min (i.e., carnosine±inhibitors, pH-dependent and concentration-dependent studies).

DISCUSSION

Carnosine, a naturally-occurring dipeptide and dietary supplement, has been shown to have some renoprotective qualities (23–26) yet no studies have delineated its mechanism of transport in kidney. In the present study, several new findings were revealed with respect to the transport mechanisms of carnosine in SKPT cells. Specifically, we have demonstrated that: (1) PEPT2 is the only peptide transporter responsible for the apical uptake of carnosine; the basolateral transporter is saturable, inhibited by dipeptide/mimetic substrates but non-concentrative, thereby, suggesting a facilitative carrier, (2) PHT1 mRNA is expressed in rat kidney lysates and SKPT monolayers, however, this peptide/histidine transporter is functionally inactive at both the apical and basolateral membranes of the cell, and (3) the apical-to-basolateral transepithelial transport of carnosine is severely rate-limited by its cellular efflux across the basolateral membrane (i.e., CL_{CB}/CL_{AC} ratio=0.004). In contrast, the basolateral-to-apical transepithelial transport of carnosine is rate-limited to a minor extent by its cellular influx at the basolateral membrane (i.e., CL_{BC}/CL_{CA} ratio=0.8). Thus, the directionality of transcellular kinetics can more fully be appreciated by understanding all of the influx and efflux parameters for a given substrate in the cellular compartment model (Fig. 1).

Our findings regarding the influx and efflux clearances of carnosine in SKPT cells are in agreement with studies using GlySar as a model substrate in this cell line. In particular, Bravo *et al.* (37) reported similar apical-to-basolateral and basolateral-to-apical fluxes of GlySar even though the apical uptake of dipeptide was about five times greater than its basolateral uptake in SKPT cells. In the study by Neumann *et al.* (38) the transepithelial apical-to-basolateral flux of GlySar was only 28% higher than its reverse flux (i.e., basolateral to apical direction) in SKPT cells despite the apical uptake of GlySar being about 3.5 times greater than its basolateral uptake. The values in our study were twofold and 15-fold, respectively, for the preferential basolateral-to-apical flux (Fig. 3B) and apical intracellular accumulation (Fig. 3A) of carnosine. To account for the anomaly between transcellular transport and apical uptake, Bravo *et al.* (37) speculated that a low basolateral transport activity may limit the carrier-mediated transepithelial flux of GlySar in SKPT cells. Our kinetic analysis agrees with this assessment and has demonstrated that carnosine is effluxed at a much slower rate across the basolateral *versus* apical membrane of SKPT cells (Fig. 3C).

The efflux studies suggest that once carnosine enters the epithelial cells of kidney proximal tubule from the luminal side, the dipeptide accumulates substantially within the cell rather than being transported to the blood side. Carnosine may then recycle back to the luminal compartment. Our results show that carnosine has an 11 times greater concentration in SKPT cells as compared to medium and that its cell-to-apical efflux is about ten times greater than the substrate's

cell-to-basolateral efflux. We reported a similar finding for carnosine in rat choroid plexus primary cell cultures (28), where its intracellular to extracellular concentration ratio was approximately 135 to 1 and apical efflux was about four times greater than basolateral efflux.

The SKPT cell line, derived from rat kidney proximal tubule cells, has been used previously as a model system to study the mechanism of peptide/mimetic transport in epithelial cells of kidney proximal tubule. In this regard, functional, Northern blot and immunoblot analyses have demonstrated conclusively that SKPT cells express the high-affinity, low-capacity (i.e., "renal") peptide transporter PEPT2 but not PEPT1 (30,39,40). Moreover, confocal laser scanning microscopy showed immunostaining of PEPT2 in the apical but not basolateral membrane (41). The current study has corroborated these findings, but has also shown the functional activity of a renal basolateral peptide transporter in SKPT cells (Figs. 4B, 5B and 6B) and the presence of the peptide/histidine transporter PHT1 in this cell line as well as rat kidney lysates (Fig. 2). While several studies have reported on the accumulation of GlySar in SKPT cells (39,40,42–45), only apical uptake was investigated and a non-physiologic, synthetic dipeptide was used as a model substrate. Moreover, the potential roles of the renal basolateral peptide transporter and PHT1 were not appreciated at that time and, as a result, studies were not appropriately designed to probe whether or not other peptide transporters might be involved in renal trafficking of peptides at the plasma membrane.

The high-affinity uptake of carnosine at the apical membrane of SKPT cells (i.e., $K_m=49 \mu\text{M}$) is comparable to the PEPT2-mediated uptake of carnosine in rat choroid plexus primary cell cultures ($K_m=34 \mu\text{M}$) (28) and whole tissue ($K_m=39 \mu\text{M}$) (46), and rat neonatal astrocytes ($K_m=43 \mu\text{M}$) (47). This finding, along with the proton-dependence, concentration-dependence and inhibitor specificity of carnosine in SKPT monolayers, supports the contention that PEPT2 is responsible for its uptake at the apical surface of these cells. On the other hand, the saturable but non-concentrative uptake of carnosine at the basolateral membrane, along with its preferred uptake over efflux at this membrane (i.e., CL_{BC}/CL_{CB} ratio=32), would suggest that the basolateral transporter of carnosine is facilitative in the inward direction. Based on functional experiments in MDCK cells, Inui and coworkers (16,18,48) reported that the renal basolateral peptide transporter was distinct from that of known peptide transporters (i.e., PEPT1 and PEPT2) and the intestinal basolateral peptide transporter. They also suggested that the basolateral peptide transporter was facilitative and that it was involved in the cellular uptake, but not cellular efflux, of small peptides in the MDCK cell line. MDCK cells, however, display features of distal tubules or collecting ducts (49) as opposed to proximal tubules where peptide reabsorption occurs (4). Moreover, although MDCK cells express a proton-peptide cotransporter at the apical membrane, its kinetic characteristics are that of PEPT1 and not PEPT2 (39). As a result, the SKPT cell line appears to have greater relevance to peptide transport in kidney. Notwithstanding these differences in experimental model, the precise nature of the renal basolateral transporter is uncertain as long as the clone of this protein remains unavailable.

In conclusion, despite the substantial cellular uptake of carnosine by PEPT2 at the apical membrane, this dipeptide is expected to have minimal tubular reabsorption into blood due to its very limited efflux across the basolateral membrane. This is important because, once inside the cell, carnosine may accumulate (as intact dipeptide or constituent amino acids) and have beneficial renoprotective properties. Although cellular uptake of carnosine at the renal basolateral transporter is fairly low when compared to luminal uptake, secretion across the cell may be possible, although minor, because of its favorable efflux kinetics at the apical membrane. These findings elucidate, for the first time, a complete picture of the cellular kinetics of carnosine in SKPT cells and, more importantly, the influence of influx and efflux clearances on transepithelial transport. Future studies will be performed with carnosine in wild-type and PEPT2 null mice to further probe the *in vivo* pharmacokinetics, tissue distribution and renal handling of this naturally-occurring dipeptide and dietary nutrient supplement.

ACKNOWLEDGMENTS

This work was supported in part by Grants R01 GM035498 (D.E.S.) and R01 NS034709 (R.F.K.) from the National Institutes of Health.

REFERENCES

- H. Daniel, and G. Kottra. The proton oligopeptide cotransporter family SLC15 in physiology and pharmacology. *Pflugers Arch.* **447**:610–618 (2004) doi:10.1007/s00424-003-1101-4.
- D. Herrera-Ruiz, and G.T. Knipp. Current perspectives on established and putative mammalian oligopeptide transporters. *J. Pharm. Sci.* **92**:691–714 (2003) doi:10.1002/jps.10303.
- Y. J. Fei, Y. Kanai, S. Nussberger, V. Ganapathy, F. H. Leibach, M. F. Romero, S. K. Singh, W. F. Boron, and M. A. Hediger. Expression cloning of a mammalian proton-coupled oligopeptide transporter. *Nature.* **368**:563–566 (1994) doi:10.1038/368563a0.
- H. Shen, D. E. Smith, T. Yang, Y. G. Huang, J. B. Schnermann, and F. C. Brosius 3rd. Localization of PEPT1 and PEPT2 proton-coupled oligopeptide transporter mRNA and protein in rat kidney. *Am. J. Physiol.* **276**:F658–F665 (1999).
- D. A. Groneberg, F. Döring, P. R. Eynott, A. Fischer, and H. Daniel. Intestinal peptide transport: Ex vivo uptake studies and localization of peptide carrier PEPT1. *Am. J. Physiol. Gastrointest. Liver Physiol.* **281**:G697–G704 (2001).
- W. Liu, R. Liang, S. Ramamoorthy, Y. J. Fei, M. E. Ganapathy, M. A. Hediger, V. Ganapathy, and F. H. Leibach. Molecular cloning of PEPT 2, a new member of the H⁺/peptide cotransporter family, from human kidney. *Biochim. Biophys. Acta.* **1235**:461–466 (1995) doi:10.1016/0005-2736(95)80036-F.
- I. Rubio-Aliaga, M. Boll, and H. Daniel. Cloning and characterization of the gene encoding the mouse peptide transporter PEPT2. *Biochem. Biophys. Res. Commun.* **276**:734–741 (2000) doi:10.1006/bbrc.2000.3546.
- D. A. Groneberg, F. Döring, S. Theis, M. Nickolaus, A. Fischer, and H. Daniel. Peptide transport in the mammary gland: expression and distribution of PEPT2 mRNA and protein. *Am. J. Physiol. Endocrinol. Metab.* **282**:E1172–E1179 (2002).
- K. Inui, T. Terada, S. Masuda, and H. Saito. Physiological and pharmacological implications of peptide transporters, PEPT1 and PEPT2. *Nephrol. Dial. Transplant.* **15**(Suppl 6):11–13 (2000) doi:10.1093/ndt/15.suppl_6.11.
- S.M. Ocheltree, H. Shen, Y. Hu, R.F. Keep, and D.E. Smith. Role and relevance of peptide transporter 2 (PEPT2) in the kidney and choroid plexus: *in vivo* studies with glycylsarcosine in wild-type and PEPT2 knockout mice. *J. Pharmacol. Exp. Ther.* **315**:240–247 (2005) doi:10.1124/jpet.105.089359.
- H. Shen, S. M. Ocheltree, Y. Hu, R. F. Keep, and D. E. Smith. Impact of genetic knockout of PEPT2 on cefadroxil pharmacokinetics, renal tubular reabsorption and brain penetration in mice. *Drug Metab. Dispos.* **35**:1209–1216 (2007).
- K. Takahashi, N. Nakamura, T. Terada, T. Okano, T. Futami, H. Saito, and K. I. Inui. Interaction of beta-lactam antibiotics with H⁺/peptide cotransporters in rat renal brush-border membranes. *J. Pharmacol. Exp. Ther.* **286**:1037–1042 (1998).
- T. Yamashita, S. Shimada, W. Guo, K. Sato, E. Kohmura, T. Hayakawa, T. Takagi, and M. Tohyama. Cloning and functional expression of a brain peptide/histidine transporter. *J. Biol. Chem.* **272**:10205–10211 (1997) doi:10.1074/jbc.272.17.11408.
- K. Sakata, T. Yamashita, M. Maeda, Y. Moriyama, S. Shimada, and M. Tohyama. Cloning of a lymphatic peptide/histidine transporter. *Biochem. J.* **356**:53–60 (2001) doi:10.1042/0264-6021:3560053.
- T. Terada, K. Sawada, H. Saito, Y. Hashimoto, and K. Inui. Functional characteristics of basolateral peptide transporter in the human intestinal cell line Caco-2. *Am. J. Physiol.* **276**:G1435–G1441 (1999).
- T. Terada, K. Sawada, T. Ito, H. Saito, Y. Hashimoto, and K. Inui. Functional expression of novel peptide transporter in renal basolateral membranes. *Am. J. Physiol. Renal. Physiol.* **279**:F851–F857 (2000).
- M. Irie, T. Terada, M. Okuda, and K. Inui. Efflux properties of basolateral peptide transporter in human intestinal cell line Caco-2. *Pflugers Arch.* **449**:186–194 (2004) doi:10.1007/s00424-004-1326-x.
- K. Sawada, T. Terada, H. Saito, and K. Inui. Distinct transport characteristics of basolateral peptide transporters between MDCK and Caco-2 cells. *Pflugers Arch.* **443**:31–37 (2001) doi:10.1007/s004240100669.
- O. I. Aruoma, M. J. Laughton, and B. Halliwell. Carnosine, homocarnosine and anserine: could they act as antioxidants *in vivo*? *Biochem. J.* **264**:863–869 (1989).
- P. E. Hartman, Z. Hartman, and K. T. Ault. Scavenging of singlet molecular oxygen by imidazole compounds: high and sustained activities of carboxy terminal histidine dipeptides and exceptional activity of imidazole-4-acetic acid. *Photochem. Photobiol.* **51**:59–66 (1990) doi:10.1111/j.1751-1097.1990.tb01684.x.
- A. R. Hipkiss, J. E. Preston, D. T. Himsworth, V. C. Worthington, M. Keown, J. Michaelis, J. Lawrence, A. Mateen, L. Allende, P. A. Eagles, and N. J. Abbott. Pluripotent protective effects of carnosine, a naturally occurring dipeptide. *Ann. N. Y. Acad. Sci.* **854**:37–53 (1998) doi:10.1111/j.1749-6632.1998.tb09890.x.
- A. R. Hipkiss. Carnosine, a protective, anti-ageing peptide? *Int. J. Biochem. Cell Biol.* **30**:863–868 (1998) doi:10.1016/S1357-2725(98)00060-0.
- B. Janssen, D. Hohenadel, P. Brinkkoetter, V. Peters, N. Rind, C. Fischer, I. Rychlik, M. Cerna, M. Romzova, E. de Heer, H. Baelde, S. J. Bakker, M. Ziric, E. Rondeau, P. Mathieson, M. A. Saleem, J. Meyer, H. Koppel, S. Sauerhoefer, C. R. Bartram, P. Nawroth, H. P. Hammes, B. A. Yard, J. Zschocke, and F. J. van der Woude. Carnosine as a protective factor in diabetic nephropathy: association with a leucine repeat of the carnosinase gene CNDP1. *Diabetes.* **54**:2320–2327 (2005) doi:10.2337/diabetes.54.8.2320.
- T. Fujii, M. Takaoka, T. Muraoka, H. Kurata, N. Tsuruoka, H. Ono, Y. Kiso, T. Tanaka, and Y. Matsumura. Preventive effect of L-carnosine on ischemia/reperfusion-induced acute renal failure in rats. *Eur. J. Pharmacol.* **474**:261–267 (2003) doi:10.1016/S0014-2999(03)02079-X.
- T. Fujii, M. Takaoka, N. Tsuruoka, Y. Kiso, T. Tanaka, and Y. Matsumura. Dietary supplementation of L-carnosine prevents ischemia/reperfusion-induced renal injury in rats. *Biol. Pharm. Bull.* **28**:361–363 (2005) doi:10.1248/bpb.28.361.
- H. Kurata, T. Fujii, H. Tsutsui, T. Katayama, M. Ohkita, M. Takaoka, N. Tsuruoka, Y. Kiso, Y. Ohno, Y. Fujisawa, T. Shokoji, A. Nishiyama, Y. Abe, and Y. Matsumura. Renoprotective effects of l-carnosine on ischemia/reperfusion-induced renal injury in rats. *J. Pharmacol. Exp. Ther.* **319**:640–647 (2006) doi:10.1124/jpet.106.110122.
- D. O. Son, H. Satsu, Y. Kiso, and M. Shimizu. Characterization of carnosine uptake and its physiological function in human intestinal epithelial Caco-2 cells. *Biofactors.* **21**:395–398 (2004).

28. N. S. Teuscher, H. Shen, C. Shu, J. Xiang, R. F. Keep, and D. E. Smith. Carnosine uptake in rat choroid plexus primary cell cultures and choroid plexus whole tissue from PEPT2 null mice. *J. Neurochem.* **89**:375–382 (2004) doi:10.1111/j.1471-4159.2004.02333.x.
29. R. K. Bhardwaj, D. Herrera-Ruiz, N. Eltoukhy, M. Saad, and G. T. Knipp. The functional evaluation of human peptide/histidine transporter 1 (hPHT1) in transiently transfected COS-7 cells. *Eur. J. Pharm. Sci.* **27**:533–542 (2006) doi:10.1016/j.ejps.2005.09.014.
30. C. Shu, H. Shen, U. Hopfer, and D. E. Smith. Mechanism of intestinal absorption and renal reabsorption of an orally active ACE inhibitor: uptake and transport of fosinopril in cell cultures. *Drug Metab. Dispos.* **29**:1307–1315 (2001).
31. N. S. Teuscher, A. Novotny, R. F. Keep, and D. E. Smith. Functional evidence for presence of PEPT2 in rat choroid plexus: studies with glycylsarcosine. *J. Pharmacol. Exp. Ther.* **294**:494–499 (2000).
32. C. Shu, H. Shen, N. S. Teuscher, P. J. Lorenzi, R. F. Keep, and D. E. Smith. Role of PEPT2 in peptide/mimetic trafficking at the blood–cerebrospinal fluid barrier: studies in rat choroid plexus epithelial cells in primary culture. *J. Pharmacol. Exp. Ther.* **301**:820–829 (2002) doi:10.1124/jpet.301.3.820.
33. R. F. Kletzien, M. W. Pariza, J. E. Becker, and V. R. Potter. A method using 3-O-methyl-D-glucose and phloretin for the determination of intracellular water space of cells in monolayer culture. *Anal. Biochem.* **68**:537–544 (1975) doi:10.1016/0003-2697(75)90649-1.
34. A. S. Pollock, D. G. Warnock, and G. J. Strewler. Parathyroid hormone inhibition of $\text{Na}^+\text{-H}^+$ antiporter activity in a cultured renal cell line. *Am. J. Physiol.* **250**:F217–F225 (1986).
35. H. Sun, and K. S. Pang. Permeability, transport, and metabolism of solutes in Caco-2 cell monolayers: A theoretical study. *Drug Metab. Dispos.* **35**:102–123 (2008).
36. C. U. Nielsen, C. T. Supuran, A. Scozzafava, S. Frokjaer, B. Steffansen, and B. Brodin. Transport characteristics of L-carnosine and the anticancer derivative 4-toluenesulfonylurido-carnosine in a human epithelial cell line. *Pharm. Res.* **19**:1337–1344 (2002) doi:10.1023/A:1020306926419.
37. S. A. Bravo, C. U. Nielsen, S. Frokjaer, and B. Brodin. Characterization of rPEPT2-mediated Gly-Sar transport parameters in the rat kidney proximal tubule cell line SKPT-0193 cl.2 cultured in basic growth media. *Mol. Pharmaceutics* **2**:98–108 (2005) doi:10.1021/mp049892q.
38. J. Neumann, M. Bruch, S. Gebauer, and M. Brandsch. Transport of the phosphonodipeptide alafosfalin by the H⁺/peptide cotransporters PEPT1 and PEPT2 in intestinal and renal epithelial cells. *Eur. J. Biochem.* **271**:2012–2017 (2004) doi:10.1111/j.1432-1033.2004.04114.x.
39. M. Brandsch, C. Brandsch, P. D. Prasad, V. Ganapathy, U. Hopfer, and F. H. Leibach. Identification of a renal cell line that constitutively expresses the kidney-specific high-affinity H⁺/peptide cotransporter. *FASEB J.* **9**:1489–1496 (1995).
40. M. E. Ganapathy, M. Brandsch, P. D. Prasad, V. Ganapathy, and F. H. Leibach. Differential recognition of beta-lactam antibiotics by intestinal and renal peptide transporters, PEPT 1 and PEPT 2. *J. Biol. Chem.* **270**:25672–25677 (1995) doi:10.1074/jbc.270.43.25672.
41. S. A. Bravo, C. U. Nielsen, J. Amstrup, S. Frokjaer, and B. Brodin. Epidermal growth factor decreases PEPT2 transport capacity and expression in the rat kidney proximal tubule cell line SKPT0193 cl.2. *Am. J. Physiol. Renal. Physiol.* **286**:F385–F393 (2004) doi:10.1152/ajprenal.00226.2003.
42. M. E. Ganapathy, W. Huang, H. Wang, V. Ganapathy, and F. H. Leibach. Valacyclovir: a substrate for the intestinal and renal peptide transporters PEPT1 and PEPT2. *Biochem. Biophys. Res. Commun.* **246**:470–475 (1998) doi:10.1006/bbrc.1998.8628.
43. M. E. Ganapathy, P. D. Prasad, B. Mackenzie, V. Ganapathy, and F. H. Leibach. Interaction of anionic cephalosporins with the intestinal and renal peptide transporters PEPT 1 and PEPT 2. *Biochim. Biophys. Acta.* **1324**:296–308 (1997) doi:10.1016/S0005-2736(96)00234-9.
44. M. Brandsch, C. Brandsch, M. E. Ganapathy, C. S. Chew, V. Ganapathy, and F. H. Leibach. Influence of proton and essential histidyl residues on the transport kinetics of the H⁺/peptide cotransport systems in intestine (PEPT 1) and kidney (PEPT 2). *Biochim. Biophys. Acta.* **1324**:251–262 (1997) doi:10.1016/S0005-2736(96)00231-3.
45. M. Sugawara, W. Huang, Y. J. Fei, F. H. Leibach, V. Ganapathy, and M. E. Ganapathy. Transport of valganciclovir, a ganciclovir prodrug, via peptide transporters PEPT1 and PEPT2. *J. Pharm. Sci.* **89**:781–789 (2000) doi:10.1002/(SICI)1520-6017(200006)89:6<781::AID-JPS10>3.0.CO;2-7.
46. N. S. Teuscher, R. F. Keep, and D. E. Smith. PEPT2-mediated uptake of neuropeptides in rat choroid plexus. *Pharm. Res.* **18**:807–813 (2001) doi:10.1023/A:1011088413043.
47. J. Xiang, Y. Hu, D. E. Smith, and R. F. Keep. PEPT2-mediated transport of 5-aminolevulinic acid and carnosine in astrocytes. *Brain Res.* **1122**:18–23 (2006) doi:10.1016/j.brainres.2006.09.013.
48. T. Terada, and K. Inui. Peptide transporters: structure, function, regulation and application for drug delivery. *Curr. Drug Metab.* **5**:85–94 (2004) doi:10.2174/1389200043489153.
49. J. S. Handler. Studies of kidney cells in culture. *Kidney Int.* **30**:208–215 (1986) doi:10.1038/ki.1986.173.